Single Molecule Dynamics Associated with Protein Folding and Deformations of Light-Harvesting Complexes.

David S. Talaga*‡, Yiwei Jia*, Martin A. Bopp*, Alexander Sytnik*, William A. DeGrado#, Richard J. Cogdell† and Robin M. Hochstrasser*∗

*Chemistry Department and NIH Laser Resource, University of Pennsylvania, Philadelphia, PA, 19104, USA
#Department of Biochemistry and Biophysics, University of Pennsylvania
†Division of Biochemistry and Molecular Biology, Institute of Biomedical and Life Sciences, University of Glasgow, Glasgow, G12 8QQ, UK
‡Department of Chemistry and Chemical Biology, Rutgers, The State University of New Jersey, New Brunswick/Piscataway, NJ 08854†

(Dated: February 5, 2002)

Two new applications of single molecule methods in biology are described. In one, single assemblies of the intact light harvesting complex LH2 from Rhodopseudomonas acidophila were bound to mica surfaces at 300K and examined by observing their fluorescence after polarized light excitation. They mostly behaved as electrically elliptic absorbers whose ellipticity fluctuates, showing that there is a mobile structural deformation. The other application involves the folding and unfolding of a coiled coil GCN4-P1 peptides. By following the trajectory of individual members of a folding ensemble we are able to evaluate of men and distributions of properties not available from bulk studies.

Keywords:

I. INTRODUCTION

Experimental understanding of biological and chemical systems is based primarily on measurements of many molecules and therefore the evolution of the mean of that ensemble. However, since heterogeneity of structure and mechanism is required to describe complex systems such as proteins and other biological assemblies, this useful paradigm can break down. Recent developments in single molecule detection have allowed the study of single molecules and single biological assemblies under physiological conditions. By following the trajectory of individual members of an equilibrium ensemble as they evolve in time fluctuation rates, reaction rate constants, and distributions of other properties can be evaluated.

We present two applications of single molecule spectroscopy that illustrate how ensemble averaging masks important dynamic properties fluctuating systems. In the first, mobile elliptical structural deformations are observed in single assemblies of the light harvesting complex, LH2. These mobile structural deformations are averaged in bulk measurements resulting in the erroneous conclusion that LH2 is a circular absorber. In the second application trajectories of individual members of a folding ensemble of coiled coil GCN4-P1 peptides allow us to determine distributions of properties not available from bulk studies.

∗Electronic address: hochstra@sas.upenn.edu, talaga@rutgers.edu
†URL: http://talaga.rutgers.edu

II. STRUCTURAL DEFORMATIONS OF SURFACE-IMMOBILIZED SINGLE LIGHT-HARVESTING COMPLEXES.[1]

The crystal structure of the LH2 complex from photosynthetic bacteria Rhodopseudomonas acidophila is notable for its high symmetry arrangement of the nine $\alpha\beta$-dipeptides which form the scaffold holding the associated bacteriochlorophyll (Bchl) cofactors.[2] The LH2 Bchls are arranged into two rings that have approximate 9-fold rotation symmetry. The B800 ring contains nine monomeric Bchls located between the β-apoproteins. The B850 ring consists of nine pairs of Bchls each associated with one $\alpha\beta$-dipeptide. In the LH2 complex the B800 ring absorbs light and transfers the excitation energy to B850 in less than a picosecond.[3] The excitation properties of macromolecular systems depend on the interplay between the nuclear motions that tend to localize excitations, and the delocalizing effect of the interaction between the molecules.[4] Therefore the nature of the excitation and energy transfer in the LH2 complex must depend not only on the static or average structure but also on the structural fluctuations that can occur in bacterial membrane. Single molecule methods are well suited for the investigation of the microseconds to seconds structural dynamics.[5] Previously we[6] and others[7] applied single molecule confocal microscopy for the photophysical and photochemical characterization of the LH2 complexes.

The LH2 complexes were immobilized on a mica surface to model the protein interactions occurring in bacterial cells. The mica has some nega-

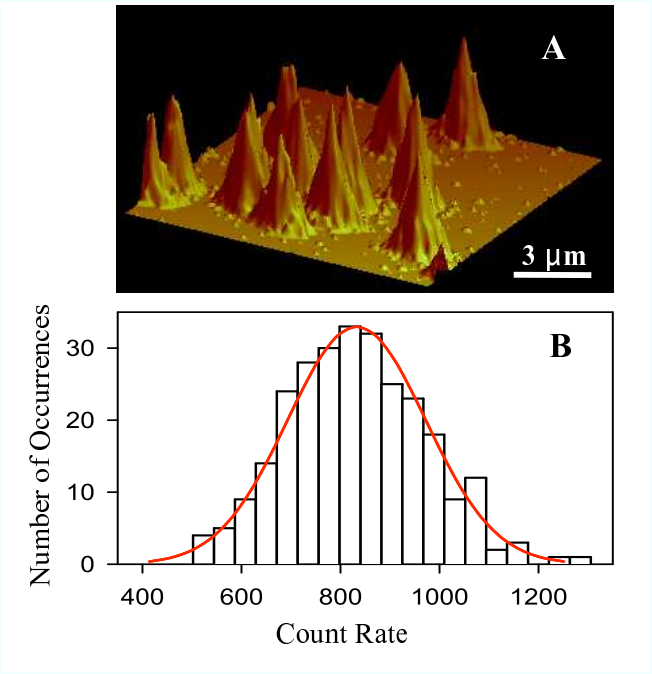

FIG. 1 The fluorescence images of single mica-bound LH2 complexes excited with circularly polarized light at 794 nm (A) and the distribution of the fluorescence count rates of the 273 single LH2s fitted with a Gaussian function with a mean = 833, and σ = 140 counts (B). The buffer is 50 mM Tris·HCl, pH 7.8/0.1% lauryldimethylamine oxide.

tive charges on its atomically flat surface but it can also have hydrophobic interactions with the protein. The N-terminal regions of LH2 are largely negatively charged because of 27 glutamates and should avoid the mica surface. As a result, the LH2 is expected to be bound to the mica via C-termini. In that case the B850 ring will be closest to the surface.

The fluorescence images and trajectories were recorded on a confocal microscope1 on samples deoxygenated by an enzymatic system. Because the transition dipoles for B850 and B800 both lie in the xy-plane of the LH2 complex,[8] both B850 and B800 should behave as essentially circular oscillators with the same absorption cross section for all linear polarizations in the xy-plane (x, y, z are the molecule fixed coordinates with z the cylindrical axis of the assembly and X, Y, Z are the laboratory fixed coordinates with X, Y as the focal plane of the microscope.) If LH2 had the ideal circular characteristics, then its absorption cross section in circularly polarized light would depend only on the tilt angle θ between the Z-axis and the direction of light propagation, Z:

$$A_{CIRC} = \frac{1}{2}(1 + \cos^2\theta) \qquad (1)$$

For linear polarization the ideal absorption cross section also depends on the direction in the XY-plane about which tilt occurs:

$$A_\chi = \cos^2\chi + \sin^2\chi + \cos^2\theta \qquad (2)$$

where $\phi - \alpha = \chi$ is the angle in the XY-plane between the linear polarization axis α and the axis of tilt ϕ both determined with respect to X.

The total angular parts of the fluorescence signal intensities for circular and linearly polarized excitation, in the ideal case, are:

$$S_{CIRC} = \frac{1}{2}(1 + \cos^2\theta)^2 \qquad (3)$$

$$S_\chi = (\cos^2\chi + \sin^2\chi + \cos^2\theta)(1 + \cos^2\theta) \qquad (4)$$

The high sensitivity of S_{CIRC} and S_χ to the tilt angle is evident from Equations 3 and 4. When we excited the single LH2 complexes via the B800 ring (CW excitation at 794 nm) with circularly polarized light, the fluorescence images (Fig. 1A) had a narrow distribution of count rates (Fig. 1B).

The width of this distribution contains a contribution of ca. 20% from the fluorescence signal blinking, which is different for each single assembly. As shown by Equation 1, the fluorescence signals of single mica immobilized LH2 complexes excited with circularly polarized light should not depend on the azimuthal angles. Therefore, the variance in the tilt angle must be significantly less than the width of the fluorescence count rate distribution.

In the next set of experiments the 794 nm excitation light was switched between two orthogonal polarization directions X and Y at 16 Hz. The corresponding trajectories for fluorescence from B850 are labeled I_x and I_y. The total signal is $I_T = I_x + I_y$. Fig. 2A shows one fluorescence polarization trajectory having $I_x = I_y$ and constant I_T. However, it was more common to observe different signals for X and Y polarization (Fig. 2B). The fluctuations in I_x and I_y suggest that for the majority of the single LH2 complexes either the elliptic principal axes rotate in the XY-plane or the z-axis precesses about the Z-axis keeping the tilt angle constant. The total emission signal does not change during these motions. For the 78 single LH2 complexes that were investigated by the linear polarization switching 33% have similar or constantly different values of and while 67% of the single LH2 complexes undergo dynamic transformations in and on the time scale of seconds. To further characterize the anisotropic properties of Bchls we determined the average values of and for each single LH2 assembly. From these results we obtained the trajectory averaged polarization ratios, I_{minT}/I_{maxT} shown in Fig. 3A. The majority of single LH2 complexes excited at 794 nm have the ratio I_{minT}/I_{maxT}, significantly less than unity.

In contrast to the results for B800, when the single LH2 assemblies were excited with linearly polarized light at 850 nm (B850), the majority of and trajectories (67%) were very similar (e. g., Fig. 4A). A

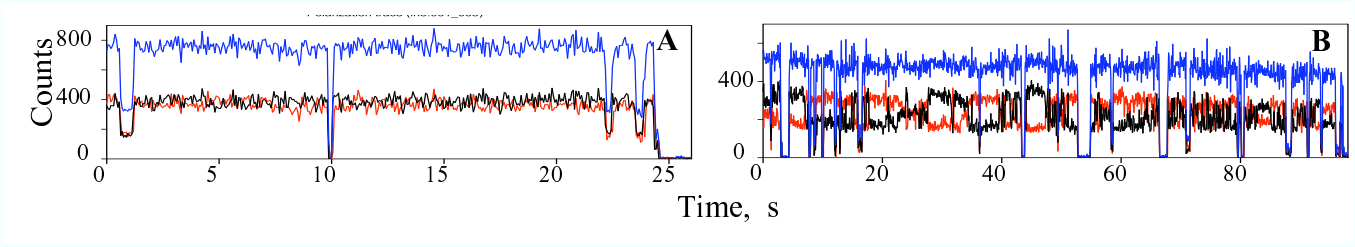

FIG. 2 The fluorescence trajectories of single LH2 complexes detected with the excitation polarization switching between 0 and π /2 at 794 nm. (A) LH2 assembly with overlapping and trajectories. (B) LH2 having substantial polarization changes. Black,; red, ; blue, the total fluorescence signal.

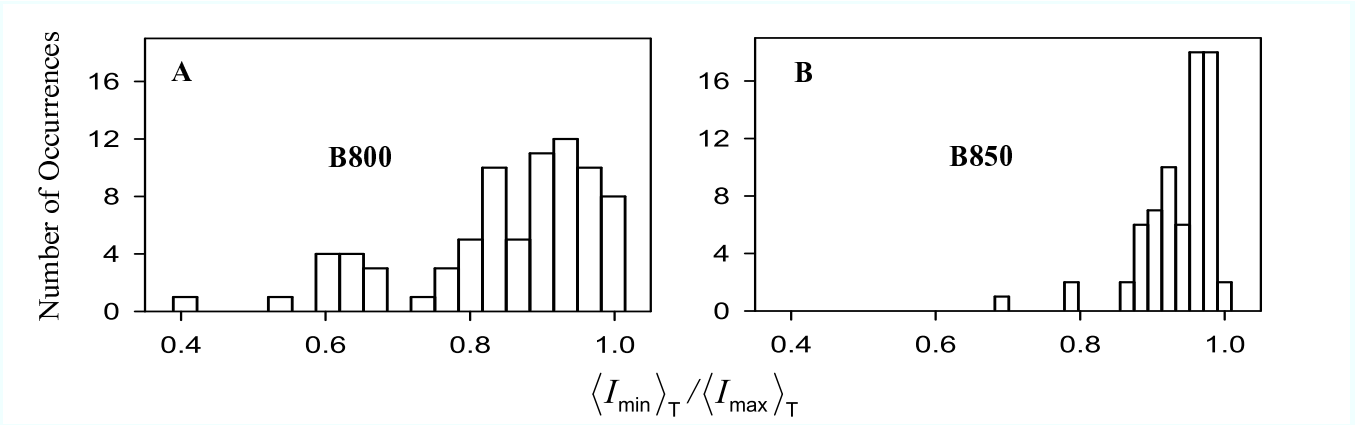

FIG. 3 The distributions of polarization ratios of single LH2 complexes determined in the polarization switching measurements. (A) $\lambda_e x$ is 794 nm. (B) $\lambda_e x$is 850 nm.

fraction (33%) of the polarization trajectories underwent fluctuations (e. g., Fig. 4B). Fig. 3B shows the IminT/ImaxT distribution for single LH2 complexes excited at 850 nm. This distribution is much narrower than the distribution at 794 nm. The majority of LH2 complexes excited via B850 had I_{minT}/I_{maxT} values close to unity indicating an apparently more circular oscillator response.

To obtain a more complete picture of the linear polarization properties we swept the 794 nm excitation over 155°. During the sweep the detected fluorescence of a single LH2 complex (S) should have the general form:

$$S = A\cos^2(\alpha + \delta) + B \qquad (5)$$

where A is an amplitude, δ is a relative phase, B is an offset, and α = 0 to 155° is the sweep angle. According to Equation 5, only B would contribute to the total fluorescence if the single LH2 assemblies were lying flat and B800 and B850 were optically ideal. Fig. 5 shows the phase and count rate trajectories of typical single LH2 complexes, determined from the detected fluorescence trajectories using Equation 5. Fig. 5A shows an example with a relatively constant δ during the whole measurement. The δ trajectory of single LH2 complex shown on Fig. 5C undergoes numerous transitions while the total count rate remains essentially constant. Fig. 6 shows the time-resolved probability histogram of the phase of this assembly. Fig. 5, B and D shows the distributions of δ for the single LH2 complexes presented on Fig. 5A and C. The data of Fig. 5 and Fig. 6 are typical of what was seen for a large number of single LH2 complexes undergoing the frequent changes in δ often in jumps of ca. 40°.

If the polarization and its dynamics were due to tilting of cylindrical LH2 there should be a correlation between the apparent ellipticity and the total signal. A statistical analysis revealed a correlation coefficient of ca. 0.28, suggesting that tilting is not the main contribution to the polarization anisotropy magnitudes or changes.

It was also found that free and mica-bound LH2 complexes have overlapping fluorescence spectra (Fig. 7A). The fluorescence peak position of the single LH2 complexes fluctuates by more than 100 cm^{-1}, and the width by over 200 cm^{-1} during the measurement. The distribution of fluorescence peaks (Fig. 7B) is peaked at 11540 cm^{-1} with a shoulder near 11460 cm^{-1}. We have suggested that the shoulder might belong to the LH2 complexes that emit from the low-

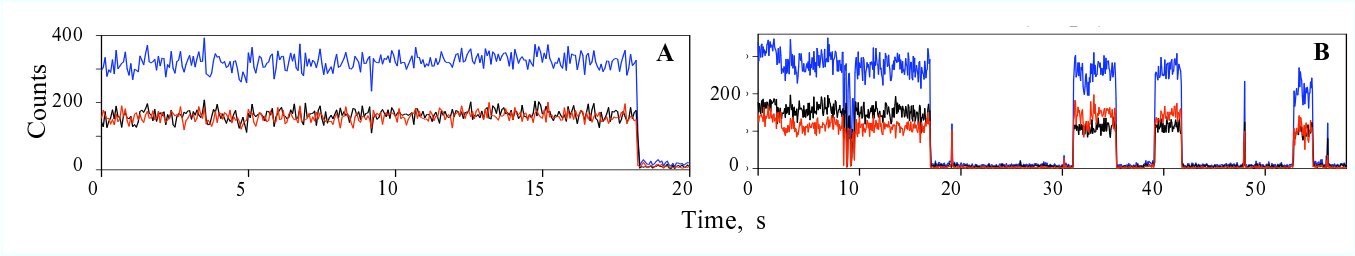

FIG. 4 The fluorescence trajectories of single LH2 complexes detected with the excitation polarization switching between 0 and π /2 at 850 nm (A) LH2 with similar and trajectories. (B) LH2 complexes undergoing fluctuations in the and signals. Black,; red, ; blue, the total fluorescence signal.

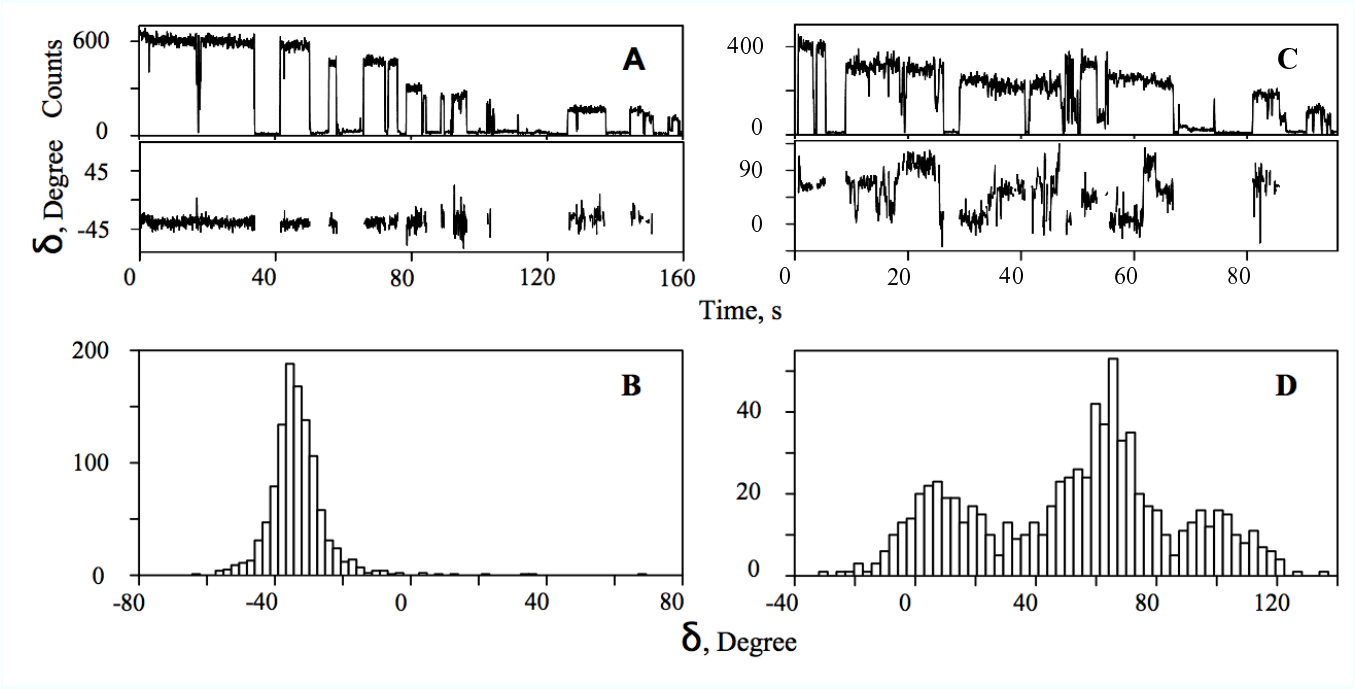

FIG. 5 The polarization asymmetry of single LH2 complexes measured by sweeping of the excitation polarization over 155°. (A) The δ and count rate trajectory of single LH2 complex with a stable δ value during the whole measurement. (B) The distribution of the δ values determined for single LH2 complex shown on (A). (C) The δ and count rate trajectory of single LH2 assembly undergoing numerous changes in δ . (D) The distribution of the δ values determined from the δ trajectory presented on (C).

est exciton level of the B850 band of states .[2,9] This transition is forbidden for the circular structure but allowed for elliptical electronic symmetry of the system.

The main results of these single molecule investigations come from the polarization switching and sweeping experiments. The circular oscillator model does not reasonably explain the data. The fact that changes in the fluorescence polarization signals are not often accompanied by changes in the total emission suggests that the fluctuations in the polarization signals of single LH2s are not caused by variations in tilt angle, but instead by variations in the ϕ angle of a tilted molecule. However, significant changes in δ are seen when the 794 nm excitation polarization is swept. In an ideal circular model this result would require all LH2 complexes to be tilted within a narrow distribution of angles. Moreover, a given single LH2 would need to undergo significant (0 140°) precession in ϕ angle without any significant changes in the θ angle. In a structural model in which immobilized LH2 complexes are dynamic, elliptic absorbers and emitters seem much more reasonable. The polarization changes seen in the experiments are therefore attributed to fluctuations of the electronic ellipticity and of the directions of the principal axes of the absorp-

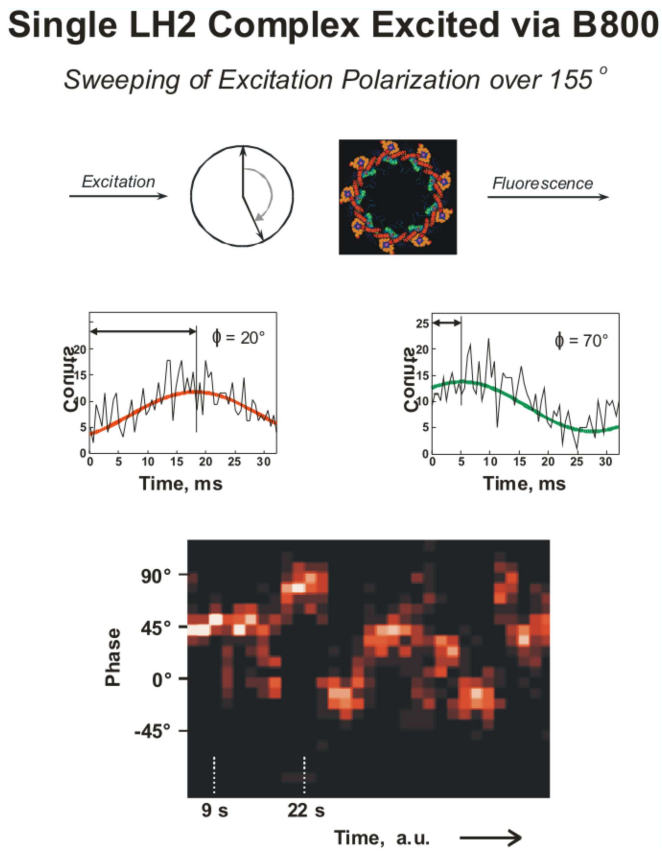

FIG. 6 The time-resolved probability histogram of the phase of single LH2 presented on Fig. 4 (A, B). The number of occurrences varies from 0 (black) to 15 (white).

tion ellipse. For LH2 an elliptical absorber is defined as having two nearly degenerate excitations with unequal transition dipoles whose vectors are fixed in the molecular frame. Any structural distortion that destroys the three-fold rotational symmetry of the B800 and/or B850 electronic states would yield an electronically elliptical absorber and emitter. The polarization sweeping measurement of δ locates the principal axes of the ellipse in the XY plane. Significant changes in δ for a single molecule are most reasonably explained by distortions occurring at different locations around the ring structures rather than by a precession around the z axis of the whole LH2 assembly. Interestingly, the phase fluctuations of ca. 2π /9 = 40° are very commonly observed in the data, as if a distortion at one location often shifts around the structure by 2π /9 steps. This picture is reasonable because a distortion of the structure near the interface between two $\alpha\beta$-dipeptides might more easily transfer to a neighboring interface, than to some random location around the ring. It is important to note that for the 155o excitation polarization sweeping eight phase peaks separated by π /9 are not observed, as would be expected if sequential distortions were occurring in a random stochastic manner around the circle of Bchls.

The different polarization behavior observed on excitation of the B800 and B850 rings (Fig. 3) suggests either a larger effect of the distortion on the electronic properties, or a larger distortion of B800 compared with B850. The B850 absorbance may be less sensitive to distortions due to its larger exciton bandwidth which implies more effective motional averaging of the distortion.[9]In addition, the B800 Bchls are held in the LH2 more peripherally than are those of B850. The B850 Bchls are each constrained by histidines of the α-, β-peptides, whereas the B800 Bchls are located between β-peptides and coordinated by the N-terminal formylmethionines of α-peptides.[2]The electronic distortion might arise from a small rotation of one or two of the B800 Bchls, and/or it could involve a partial dissociation of the assembly at the interface between two dipeptides. Although the immobilization on the mica surface may deform the structure of LH2, it is interesting that the B800 ring, which is considered to be farther from the surface than the B850 ring, seems to be the most perturbed from being a circular electronic oscillator.

III. SINGLE MOLECULE PROTEIN FOLDING TRAJECTORIES

GCN4 was studied at the single molecule level using fluorescence energy transfer between donor and acceptor dyes labeled at the N-termini of the crosslinked monomers. Distributions of fluctuating molecular structures in terms of the distance between the donor and acceptor, as inferred from the energy transfer efficiency, were measured at a series of positions in the folding equilibrium both on a modified surface and while freely diffusing in solution. Distributions of the energy transfer efficiency were obtained under both conditions permitting us to examine the folded and unfolded states and the influence of interactions with the modified surface. The time scales associated with the fluctuations that give rise to these distributions were also examined.

A peptide derived from the yeast transcription factor, GCN4, was used in this study.[10,11]The DNA binding domain of this peptide includes a sequence that forms a short segment of a two-stranded coiled coil,[12,13] as shown in Fig. 8. Coiled coils provide a very simple model system for the study of the folding of water-soluble proteins.[14–16] A peptide spanning the coiled coil of GCN4 (GCN4-P1) has been shown to form a cooperatively folded helical dimer [14,16–21]. This peptide is an excellent system for studying protein folding because it is quite simple, and yet contains a well-packed helix/helix interface, as found in globular proteins. It has been shown to exist in a two-state equilibrium between unstructured monomers and fully alpha-helical dimers.[14]The alpha-helical secondary structure and the double-helical folded

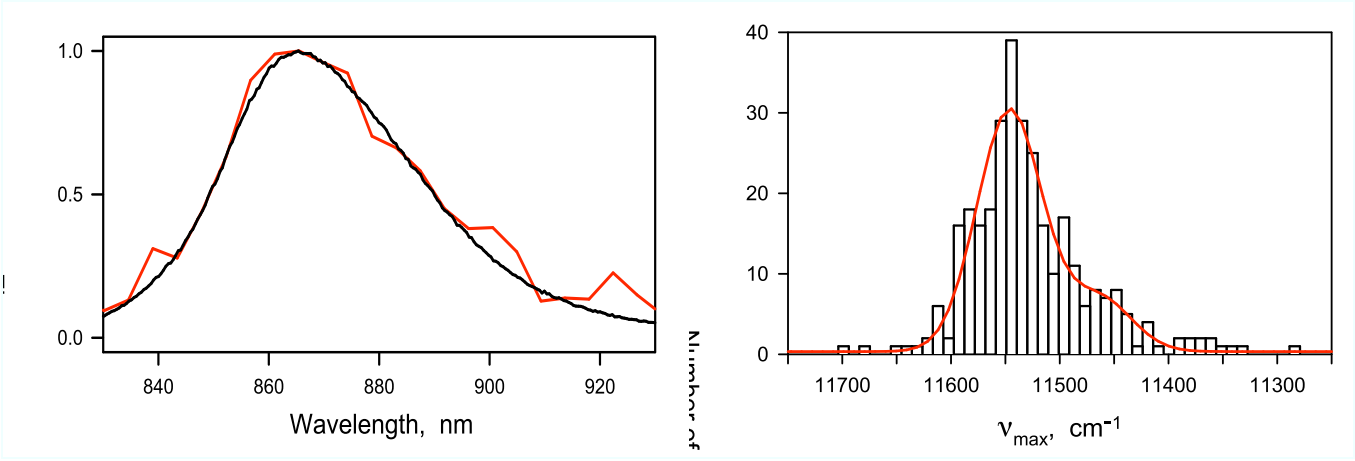

FIG. 7 (A) Conventional fluorescence spectra of free LH2 complexes (black) and emission spectrum of single mica-bound LH2 (red). (B) Distribution of the fluorescence peak positions, ?max, of single LH2 complexes and least square fit (red) to two Gaussians (mean1 = 11540 cm-1, σ1 = 30 cm^{-1}, amplitude = 30.0; mean2 = 11460 cm^{-1}, σ 2 = 30 cm^{-1}, amplitude = 6.7).

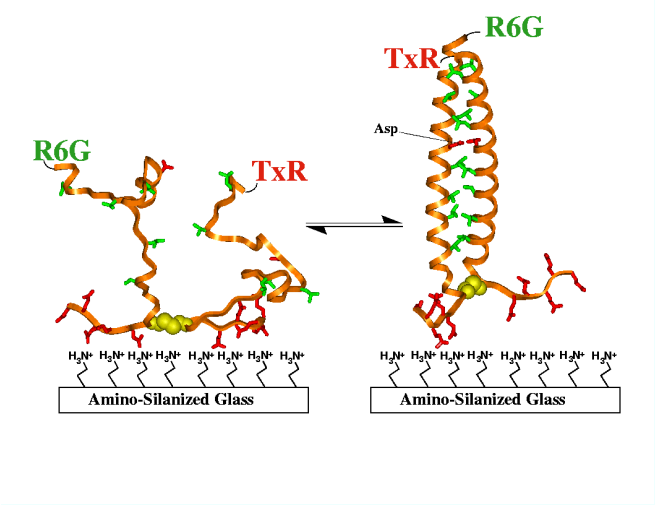

FIG. 8 Schematic representation of the folding of GCN4-Pf. The right panel shows the crystal structure of folded GCN4-P1 with a hypothetical unfolded structure at the left. The peptide adheres to the positively charged surface by electrostatic interaction with the negatively charged glutamic acids at the C terminus of the peptide. Conformational fluctuations cause changes in the donor-acceptor distance resulting in an anticorrelated modulation in the donor and acceptor fluorescence intensities.

structure apparently form concomitantly.[15−19,22] Introduction of a covalent disulfide tether between the two-peptide chains simplifies the folding reaction and thermally stabilizes GCN4, yet the peptide continues to fold in an apparent, two-state equilibrium.[23]One purpose of this study is to investigate the microscopic features of a macroscopically observed kinetic model. GCN4-P1 exhibits two-state folding kinetics when in bulk solution.[15,19] The GCN4-P1 variant employed in this study, designated GCN4-Pf,11 has the sequence GGRMKQLEDK[10]VEELLSKDYH[20]-LENEVARLKK[30]LVGERGGCGE[40]EEEE. (Fig. 8) Five glutamic acid residues were appended to the C-terminus, providing a flexible appendage to allow oriented electrostatic adsorption of the peptides onto a positively charged surface for single molecule studies. Texas Red-X (TxR) was used as the energy acceptor and 5-carboxyrhodamine 6G (R6G) as the energy donor attached to the N-termini. Single molecule fluorescence intensity fluctuations can arise from a variety of photophysical sources, such as dynamic shifts in the fluorescence spectrum,[24,25] transient non-fluorescent states of the system,[26] including triplet states,[27,28] and irreversible photobleaching.[5] Angular motions of the transition dipoles of the probes R6G and TxR can contribute to the fluctuations in the present example. The relative signal intensities from donor and acceptor depend not only on the angles involved in the dipole-dipole interaction, but also on the transition dipole colatitudes, A and D. The fluctuations in A and D are expected be more correlated when GCN4-Pf is folded than when it is unfolded.

The corrected and optimally filtered trajectories are used with the quantum yields for unsensitized donor and acceptor fluoresence and energy transfer , donor and acceptor extinction coefficients to determine the quantum yield for energy transfer.

$$\Phi_{ET} = \frac{1}{1 + R/R_0} \tag{6}$$

is the ratio of the donor and acceptor extinction coefficients at the excitation wavelength. 1 is the

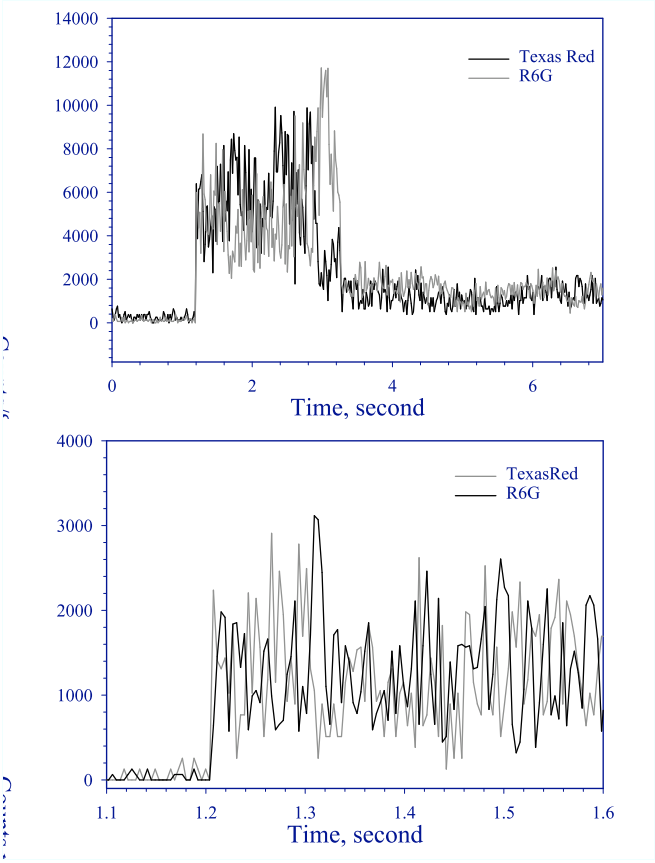

FIG. 9 High time resolution detection of donor (solid line) and acceptor (dashed line) fluorescence signals from a single GCN4-Pf molecule at pH 6.1.

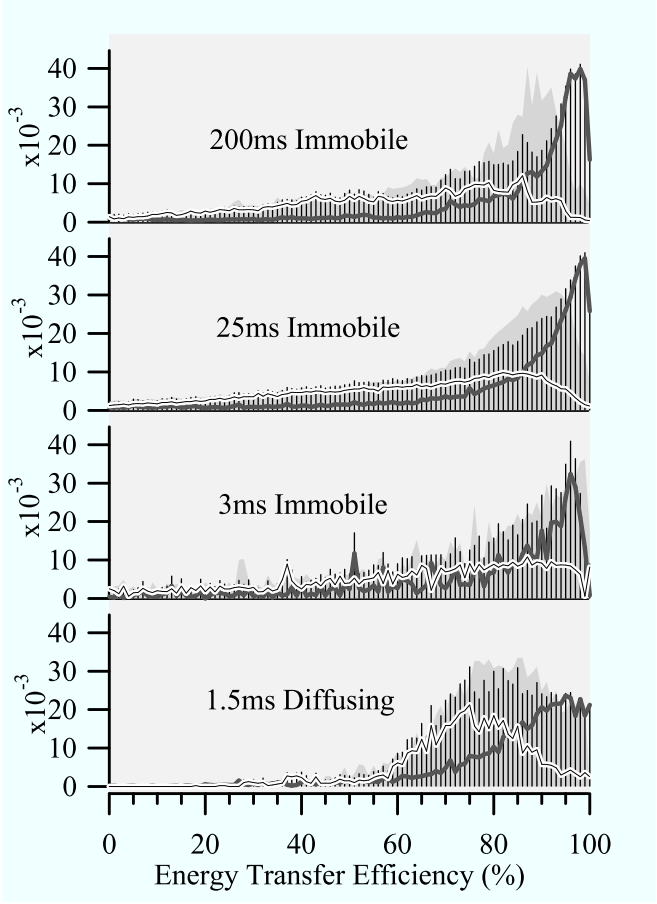

FIG. 10 This figure illustrates the distributions obtained under various conditions of denaturant vs. observation time. The filled curve represents the distribution obtained at 3 M urea. The sticks represent a linear combination of the 0 M folded distribution and the 7 M unfolded distribution shown as solid black curve and the white highlighted curve. Distributions obtained from 200 ms (a), 25 ms (b), and 3 ms (c) averaging times while immobilized on the modified surface. Part (d) shows the distributions obtained for freely diffusing GCN4 averaged for 1.5 ms.

Förster distance[29] between chromophores that gives a quantum yield for energy transfer of 50%.

The goal of this work was to measure conformational fluctuations of GCN4-Pf in the folded and unfolded states, and the dynamic equilibrium between these two conformational ensembles. Under 532 nm excitation mainly the R6G is excited, but with no urea the TxR channel shows significantly more intensity, consistent with efficient energy transfer in a folded state. At 7.4 M urea the R6G channel shows significantly more emission, indicating less effective energy transfer. The goal of this work was to measure conformational fluctuations of GCN4-Pf in the folded and unfolded states, and the dynamic equilibrium between these two conformational ensembles. Under 532 nm excitation mainly the R6G is excited, but with no urea the TxR channel shows significantly more intensity, consistent with efficient energy transfer in a folded state. At 7.4 M urea the R6G channel shows significantly more emission, indicating less effective energy transfer. We observe a number of different types of trajectories for GCN4-Pf. The acceptor signal dominates most trajectories until it photobleaching occurs, at which time the donor signal jumps to its non-perturbed level indicating that the photobleached acceptor does not act as an energy acceptor. When the donor bleaches first we see a reduction of the acceptor signal to the level of its direct excitation. Fig. 9 shows a single molecule trajectory on an expanded time scale that more clearly shows anticorrelated fluctuations in the donor and acceptor signals.

We were able to measure the donor and acceptor fluorescence intensity auto correlation and cross correlation functions. The cross correlation function is negative but its magnitude at time zero is less than the geometric mean of the amplitudes of the autocorrelation functions indicating that energy transfer is not the only mechanism for modulating the signal. Uncorrelated fluctuations of the colatitudes will in-

crease the magnitude of the autocorrelation functions whereas their correlated fluctuations will contribute to a positive cross correlation function effectively canceling some of the negative cross correlation. Nevertheless, it is clear that the signals are exhibiting dynamic modulation of the energy transfer distance.

For a given concentration of urea, the two autocorrelation functions and the cross correlation function were quite non-exponential indicating the occurrence of a range of types of structural fluctuations. This suggests that the distributions should be dependent on the time gate used in the experiment and experiments have shown this to be the case. Different portions of the distributions coalesce on different time scales. The broad feature in the 7.4 M distribution of Φ_{ET} centered at 55% does not narrow on a 25 ms gating time scale. These results show that there is a distribution of time scales for fluctuations in the energy transfer efficiency and a correlation between kinetics and structure. Fig. 10 compares the results we obtain for various observation times on the modified surface with the results for an observation time of 1.5 ms freely diffusing in solution. The broad feature at Φ_{ET}=$\sim$55% is absent in the freely diffusing distribution. Therefore we attribute this portion of the unfolded ensemble to slowly interconverting frustrated peptides interacting with the surface. Apart from the broad feature in the 7 M distribution on the surface, we see that the distributions observed on the surface and the freely diffusing in solution are quite similar leading us to conclude that the main peak in the distribution, which is substantially broader than shot noise, is representative of the freely fluctuating peptide.

Acknowledgments

This research was supported by the National Institutes of Health and the National Science Foundation, with instrumentation developed under National Institutes of Health Grant RR03148 (R.M.H.); by the Biotechnology and Biological Sciences Research Council, U.K. (R.J.C.).

References

(1) Bopp, M. A.; Sytnik, A.; Howard, T. D.; Cogdell, R. J.; Hochstrasser, R. M. Proc. Natl. Acad. Sci 1999, 96, 11271-11276.

(2) McDermott, G.; Prince, S. M.; Freer, A. A.; Hawthornthwaite-Lawless, A. M.; Papiz, M. Z.; Cogdell, R. J.; Isaacs, N. W. Nature (London) 1995, 374, 517-521.

(3) Sundstroḿ, V.; Pullerits, T.; Van Grondelle, R. J. Phys. Chem. B 1999, 103, 2327-2346.

(4) Davydov, A. S. Theory of Molecular Excitons; Plenum: New York, 1971.

(5) Xie, X. S.; Trautman, J. K. Annu. Rev. Phys. Chem. 1998, 49, 441-480.

(6) Bopp, M. A.; Jia, Y.; Li, L.; Cogdell, R. J.; Hochstrasser, R. M. Proc. Natl. Acad. Sci. Usa 1997, 94, 10630-10635.

(7) van Oijen, A. M.; Ketelaars, M.; Kohler, J.; Aartsma, T. J.; Schmidt, J. J. Phys. Chem. B 1998, 102, 9363-9366.

(8) Freer, A. A.; Prince, S. M.; Sauer, K.; Papiz, M.; Hawthomthwaite-Lawless, A.; Mcdermott, G.; Cogdell, R. J.; Isaacs, N. W. Structure 1996, 4, 449-462.

(9) Kumble, R.; Hochstrasser, R. M. J. Chem. Phys. 1998, 109, 855-865.

(10) Talaga, David S.; Lau, Wai Leung; Roder, H.; Tang, Jianyong; Jia, Yiwei; DeGrado, W.F.; Hochstrasser, R. M. PNAS (2000), 97, 13021-13026.

(11) Jia, Y.; Talaga, D.; Lau, W.; Lu, H.; Degrado, W.; Hochstrasser, R. Chemical Physics 1999, 247, 69-83.

(12) O'Shea, E. K.; Klemm, J. D.; Kim, P. D.; Alber, T. Science 1991, 254, 539.

(13) Ellenberger, T. E.; Brandl, C. J.; Struhl, K.; Harrison, S. C. Cell 1992, 71, 1223-1237.

(14) Lumb, K. J.; Carr, C. M.; Kim, P. S. Biochemistry 1994, 33, 7361.

(15) Sosnick, T. R.; Jackson, S.; Wilk, R. R.; Englander, S. W.; Degrado, W. F. Proteins 1996, 24, 427-32.

(16) Wendt, H.; Leder, L.; Harma, H.; Jelesarov, I.; Baici, A.; Bosshard, H. R. Biochemistry 1997, 36, 204-13.

(17) Wendt, H.; Berger, C.; Baici, A.; Thomas, R. M.; Bosshard, H. R. Biochemistry 1995, 34, 4097-107.

(18) Wendt, H.; Baici, A.; Bosshard, H. R. J. Amer. Chem. Soc. 1994, 116, 6973-74.

(19) Zitzewitz, J. A.; Bilsel, O.; Luo, J.; Jones, B. E.; Matthews, C. R. Biochemistry 1995, 34, 12812-9.

(20) Jelesarov, I.; Durr, E.; Thomas, R. M.; Bosshard, H. R. Biochemistry 1998, 37, 7539-50.

(21) Durr, E.; Jelesarov, I.; Bosshard, H. R. Biochemistry 1999, 38, 870-80.

(22) Ozeki, S.; Kato, T.; Holtzer, M. E.; Holtzer, A. Biopolymers 1991, 31, 957-66.

(23) O'shea, E. K.; Rutkowski, R.; Kim, P. S. Science 1989, 243, 538-42.

(24) Trautman, J. K.; Macklin, J. J.; Brus, L. E.; Betzig, E. Nature 1994, 369, 40.

(25) Lu, H. P.; Xie, X. S. Nature 1997, 385, 143.

(26) Ha, T.; Enderle, T.; Chemla, D. S.; Selvin, P. R.; Weiss, S. Phys. Rev. Lett. 1996, 77, 3979.

(27) Basche, T.; Kummer, S.; Brauchle, C. Nature 1995, 373, 132.

(28) Ha, T.; Enderle, T.; Chemla, D. S.; Selvin, P. R.; Weiss, S. Chem. Phys. Lett. 1997, 271, 1.

(29) Streyer, L. Ann. Rev. Biochem. 1978, 47, 819-846.